Scientific Reports

https://doi.org/10.1038/s41598-026-39547-8

Article in Press

Copper doped hybrid nanosponges functionalized with *Aplysina aerophoba* extract for enhanced bioactive performance

Received: 31 July 2025

Accepted: 5 February 2026

Published online: 09 February 2026

Cite this article as: Demirbas A., Karsli B., Uras I.S. *et al.* Copper doped hybrid nanosponges functionalized with *Aplysina aerophoba* extract for enhanced bioactive performance. *Sci Rep* (2026). https://doi.org/10.1038/s41598-026-39547-8

Ayse Demirbas, Baris Karsli, Ibrahim Seyda Uras & Belma Konuklugil

We are providing an unedited version of this manuscript to give early access to its findings. Before final publication, the manuscript will undergo further editing. Please note there may be errors present which affect the content, and all legal disclaimers apply.

If this paper is publishing under a Transparent Peer Review model then Peer Review reports will publish with the final article.

ARTICLE IN PRESS

© The Author(s) 2026. **Open Access** This article is licensed under a Creative Commons Attribution-NonCommercial-NoDerivatives 4.0 International License, which permits any non-commercial use, sharing, distribution and reproduction in any medium or format, as long as you give appropriate credit to the original author(s) and the source, provide a link to the Creative Commons licence, and indicate if you modified the licensed material. You do not have permission under this licence to share adapted material derived from this article or parts of it. The images or other third party material in this article are included in the article's Creative Commons licence, unless indicated otherwise in a credit line to the material. If material is not included in the article's Creative Commons licence and your intended use is not permitted by statutory regulation or exceeds the permitted use, you will need to obtain permission directly from the copyright holder. To view a copy of this licence, visit http://creativecommons.org/licenses/by-nc-nd/4.0/.

ARTICLE IN PRESS

Copper Doped Hybrid Nanosponges Functionalized with Aplysina aerophoba Extract for Enhanced Bioactive Performance

Ayse DEMIRBAS [1 *], Baris KARSLI [1], Ibrahim Seyda URAS [2, 3], Belma KONUKLUGIL [2, 4]

[1] Department of Seafood Processing Technology, Faculty of Fisheries, Recep Tayyip Erdogan University, 53100, Rize, TURKEY

[2] Department of Pharmacognosy, Faculty of Pharmacy, Ankara University, 06560, Ankara, TURKEY

[3] Department of Pharmacognosy, Faculty of Pharmacy, Agri Ibrahim Cecen University, 04100, Agri, TURKEY

[4] Department of Pharmacognosy, Faculty of Pharmacy, Lokman Hekim University, 06510, Ankara, TURKEY

*Corresponding author E-mail and phone: ayse.demirbas@erdogan.edu.tr, 009 0464 2233385-1440, ORCID: ID/0000-0002-7629-3263

List of ORCID ID:

İbrahim Seyda URAS: ORCID: ID/ 0000-0001-5945-8743

Baris KARSLI: ORCID: ID/ 0000-0002-3944-6988

Belma KONUKLUGIL: ORCID: ID/ 0000-0002-4753-0450

Ayse DEMIRBAS: ORCID: ID/ 0000-0002-7629-3263

List of E-mail addresses:

Ayse DEMIRBAS: ayse.demirbas@erdogan.edu.tr

Baris KARSLI: baris.karsli@erdogan.edu.tr

İbrahim Seyda URAS: isuras@agri.edu.tr

Belma KONUKLUGIL: belma.konuklugil@lokmanhekim.edu.tr

ARTICLE IN PRESS

ARTICLE IN PRESS

Abstract

In this study, Cu (II) ion incorporated hybrid nanosponge (Cu^{2+} hNSs) derived from extracts of *Aplysina aerophoba* was synthesised, and its antimicrobial activity against some bacterial species, including *Staphylococcus aureus*, *Aeromonas hydrophila*, *Aeromonas sobria*, *Escherichia coli*, and *Salmonella enterica*, was evaluated. According to the results of the characterisation test, Cu(II)-incorporated hybrid nanosponges were well dispersed on the surface. The diameters of *A. aerophoba* extract and Cu(II) ion incorporated hybrid nanosponges were found to range between 12 and 14 µm using scanning electron microscopy (SEM) for obtaining SEM images. The antioxidant activity of *A. aerophoba* extract and Cu(II) ion incorporated hybrid nanosponge was determined against 2,2-diphenyl-1-picrylhydrazyl (DPPH). Cu(II) ion-incorporated hybrid nanosponges exhibit significantly higher antimicrobial activity against *S. aureus*, *A. hydrophila*, *A. sobria*, *Escherichia coli,* and *S. enterica* compared to the *A. aerophoba* extract, which alone showed minimal activity. As a result, we suggest that Cu (II) ion incorporated hybrid nanosponges were synthesized with *A. aerophoba* extract by an effective, inexpensive, and eco-friendly method and are applicable for antimicrobial activity studies. This study demonstrates the laboratory-scale feasibility of Cu(II)-doped hybrid nanosponges functionalized with *Aplysina aerophoba* extract, providing proof-of-concept results that may serve as a foundation for future commercial applications.

Keywords: *Aplysina aerophoba*, biomaterials, green synthesis, nanosponges

1. Introduction

Aplysina aerophoba is a species of sponge in the family Aplysinidae native to the eastern Atlantic Ocean and the Mediterranean region. *Aplysina aerophoba* is reported to grow in irregular, yellow, tubular colonies up to 1 m (3 ft) wide. Additionally, the individual tubes of this species have been observed to reach 4 cm in length and 2.5 cm in width. Some small oscula, or exhalation pore, has been observed in the middle of the flattened end of each tube. Both the basal

ARTICLE IN PRESS

mass and the tubes have short, variable-length projections on their surfaces. The texture is hard and rubbery, and the surface is slick to the touch. The sponge's specific designation, "aerophoba," is derived from its proclivity to assume a blue hue when removed from its aqueous environment (Greek: "fear of air"). In 2010, it was documented that the marine *demosponge Aplysina aerophoba (Verongiida, Aplysinidae)* can serve as a source of both chitin and bioactive bromotyrosine. Currently, this sponge is cultivated in a 100 m2 marine farming facility in Kotor Bay, Montenegro, which provides a sufficient supply of both promising ingredients. Recently, for the first time, the antitumorigenic and anti-metastatic potential of bromotyrosines derived from this demosponge, such as Aeroplysinin-1 (AP1) and Isofistularin-3, was assessed on pheochromocytoma cells [1-5].

The Mediterranean sponge *A. aerophoba* is rich in brominated alkaloids, particularly isoxazoline derivatives such as aerophobins, aplysinamisine-1, and isofistularin-3, which function as chemical defenses against pathogens and predators [6-8]. These compounds display notable cytostatic, antimicrobial, and antioxidant activities [9-11], with some, such as aerophobin-1 and aeroplysinin-1, also showing promise in regenerative medicine and anticancer research [10,12]. Owing to this broad bioactivity, *A. aerophoba* has emerged as a valuable source of bioactive metabolites with potential pharmaceutical applications.

In recent years, marine-derived biomaterials such as chitosan, alginate, and sponge-derived secondary metabolites have gained attention as sustainable and functional platforms for nanotechnology. Several studies emphasize that marine-derived polysaccharides and extracts not only possess inherent bioactivity but also provide environmentally friendly templates for the synthesis of hybrid nanomaterials with applications in antimicrobial and biomedical fields [13-15].

The study of the catalytic activity of enzyme-based hybrid nanofibers (hNFs) has recently gained considerable interest. The fact that free enzymes, which are utilized in numerous sectors of the industry, are costly and unstable is a

ARTICLE IN PRESS

disadvantage. A multitude of techniques have been developed to address this issue, yet these approaches are time-consuming, expensive, and sophisticated. In general, enzymes that are rendered immobile using traditional techniques of enzyme immobilization exhibit greater stability. However, many immobilization techniques result in the partial blocking of certain enzymes' active areas, conformational changes in the enzymes, diffusion resistance between the substrate and the enzymes, and ultimately a possible decrease in the enzymes' activity [16–18]. Researchers have been engaged in the field of green synthesis, meticulously regulating the dimensions and morphology of nanoparticles, and evaluating the potential of these materials for use in biomedical and environmental applications [19]. Demirbas evaluated the antibacterial efficacy of Cu^{2+} hNSs against the FSH pathogen bacterial strain, which was produced using fruit extracts and red orange shells [20]. According to Ekennia et al., the tyrosinase-inhibiting effect of NFs was found to be diminished when ZnO-NFs were produced using *Euphorbia sanguinea* extract [21]. Al Sharie et al. demonstrated that ZnO NFs produced with *Hypericum triquetrifolium* exhibited minimum inhibitory concentrations (MIC) of 20 µg/mL against *S. aureus* and 5 µg/mL against *Enterococcus faecalis*, respectively [22]. In the same investigation, ZnO NFs were found to have anticancer action against A549 cells, which are lung cancerous [22]. The production of Cu^{2+} hNSs by *Axinyssa digitata* extract may have value in the field of antibacterial applications, as evidenced by data from another study [23]. In a study, the potential of NFs generated with an extract of *Echinophora platyloba* for wound healing was documented (*in vivo*) [24]. The same study demonstrated the antibacterial and antifungal properties of NFs against *S. aureus, E. coli*, *Trichophyton rubrum*, *Candida albicans,* and *Aspergillus niger* [24]. There is a paucity of research investigating the synthesis of hNFs employing fungal, algal, or lichen extracts, even though studies on hNF synthesis by bioreactions are somewhat limited [25-27]. To the best of our knowledge, there are no other studies that employ this algae extract-based nanomaterial synthesis method. Instead, the *Desmarestia*

ARTICLE IN PRESS

menziesii extract was solely used for the synthesis of Ag and Au metallic nanoparticles (NPs) [28]. For the first time, the macroalgae *Desmarestia menziesii* was employed as an organic component substitute for DNA and other enzymes in the synthesis of organic–inorganic hybrid NFs. Parallel to these developments, copper-based antimicrobial nanomaterials (Cu, CuO, Cu_2O, Cu-complexes, Cu-MOFs) have been extensively studied due to their broad-spectrum activity, which involves membrane disruption, ROS generation, and biofilm inhibition. Recent reports highlight their effectiveness against both Gram-positive and Gram-negative bacteria and underline their potential integration into biomedical coatings and wound healing materials [29-31]. However, challenges remain regarding cytotoxicity, controlled ion release, and long-term stability.

In this study, *A. aerophoba* extract was employed to synthesize Cu^{2+} hNSs instead of biomolecules, including proteins, enzymes, or DNA. The use of scanning electron microscopy (SEM), energy-dispersive X-ray spectroscopy (EDX), X-ray diffraction (XRD), and Fourier transform infrared spectroscopy (FT-IR) to evaluate the obtained Cu-NSs revealed the presence of antioxidant and antibacterial activity. This study provides evidence that biological extracts from plants, algae, and fungi can be used to create organic/inorganic hybrid Cu^{2+} hNSs efficiently and cost-effectively. By combining the unique biochemical environment of marine sponge-derived extracts with the well-documented antimicrobial potency of Cu nanomaterials, our work aims to provide a novel, sustainable approach to hybrid nanostructure synthesis. These findings may serve as a reference for future research in nanotechnology and related multidisciplinary studies, particularly regarding the development of cost-effective and environmentally acceptable hybrid NS syntheses and their potential applications.

2. Materials and methods

2.1. Materials and reagents

ARTICLE IN PRESS

The antimicrobial activity of *A. aerophoba* extract and nanostructure was evaluated against one strain of Gram-positive bacteria (*Staphylococcus aureus ATCC 25923*) and four strains of Gram-negative bacteria (*Aeromonas hydrophila ATCC 7966, Aeromonas sobria ATCC 43979, Escherichia coli ATCC 25922, and Salmonella enterica ATCC 13076*).

Stock cultures were subcultured for 24 hours at 37 °C on Mueller-Hinton Agar (MHA). For antimicrobial assessment, all bacterial strains were then corrected to 0.5 McFarland standard turbidity (1×10^8 CFU/mL) [32]. Each trial was run in three copies. The chemicals $CuSO_4$. $3H_2O$ and others were produced by Sigma-Aldrich.

2.2. Instrumentation and Extraction of *A. aerophoba*

The *A. aerophoba* samples were cut into small pieces (about 50g) using a knife, and each sample was then extracted four times using 500 mL of 100% methanol. Filtered merged methanol phases were vacuum evaporated till dry. The resulting dried residue was stored at 4 °C for subsequent analysis. Dry crude extract was obtained by evaporating solvents using a Buchi R–300 rotary evaporator (Switzerland). Using XRD analysis, the crystalline nature of Cu NFs was ascertained. For this, a fitted copper target was utilized to produce CuKα radiation with a wavelength of λ = 1.54056 Å to investigate Cu NFs. The XRD spectra was recorded at 2Θ angles and from 10º to 80º using CuK radiation operating at 40 kV and 30 mA. Scanning electron microscopy (SEM) was utilized to examine the phenotypic morphology, encompassing the shape, surface features, and size, of the synthesized CuNFs.

2.3. Synthesis and Characterization of Organic-Inorganic Hybrid Nanosponges Incorporating *A. aerophoba* Extract

Hybrid nanosponges were synthesized using copper(II) sulfate pentahydrate ($CuSO_4 \cdot 5H_2O$) as the inorganic precursor and an aqueous extract of *A. aerophoba* as the organic component. The formation of a blue precipitate within the reaction vessel was taken as a visual indicator of the successful development of sponge-like hybrid assemblies. Following the initial reaction, the mixture was subjected to centrifugation, after which the precipitated solids

ARTICLE IN PRESS

were redispersed in deionized water and centrifuged again to purify the product. The resulting blue material was collected, dried, and stored under appropriate conditions for subsequent analysis. The hybrid nanosponge formation is based on the well-established coordination chemistry between proteinaceous compounds and Cu(II) ions. In the early phase of the process, copper ions primarily form complexes through coordination with amino groups present in the protein molecules derived from the *A. aerophoba* extract. These complexes facilitate the nucleation of primary copper phosphate crystals. During the subsequent growth phase, these primary structures aggregate with protein molecules to form larger, coarse assemblies. Surface copper-binding sites on these aggregates promote the anisotropic growth of individual copper phosphate crystal sheets. This process leads to the development of nanostructures with pores that branch and assemble into sponge-like morphologies, hence the designation "hybrid nanosponges."

For synthesis, 1 mL of *A. aerophoba* extract (1 mg/mL) was added to 50 mL of phosphate-buffered saline (PBS, 50 mM, pH 7.4), followed by the addition of 20 mL of copper sulfate solution (120 mM). The reaction mixture was incubated at 25 °C, leading to the gradual formation of a blue precipitate at the bottom of the flask. The precipitate was collected via centrifugation at 12,000 rpm for 20 minutes and washed three times with deionized water to remove unbound components. The purified nanosponges were then subjected to comprehensive physicochemical characterization.

The morphology and elemental composition of the synthesized hybrid nanosponges were examined using scanning electron microscopy (SEM) coupled with energy-dispersive X-ray spectroscopy (EDX). SEM imaging provided high-resolution visualization of the nanostructured surfaces, utilizing a finely focused electron beam that interacts with the sample to generate various signals. These signals were detected and converted into detailed topographical images, while EDX analysis enabled both qualitative and quantitative elemental mapping, including point, line, and area scans.

ARTICLE IN PRESS

Crystalline structure analysis was performed using X-ray diffraction (XRD), a technique based on the diffraction of X-rays by periodic atomic arrangements within crystalline phases. Each crystal structure produces a characteristic diffraction pattern, functioning as a "fingerprint" for phase identification.

Fourier transform infrared spectroscopy (FTIR) was employed to assess the chemical composition of the hybrid nanosponges. This technique utilizes infrared radiation to probe the vibrational transitions of molecular bonds within the sample. The resulting absorption spectra, recorded in the range of 4000–400 cm^{-1}, serve as molecular signatures for identifying functional groups and assessing chemical interactions within the hybrid system. Following multi-step purification (centrifugation–redispersion and dialysis) and a brief EDTA rinse, FTIR/XRD showed no signatures of unreacted precursors or crystalline copper by-products, while SEM–EDX mapping confirmed homogeneous Cu distribution.

2.4. Antimicrobial activity

Antimicrobial activities of the obtained extracts and hybrid nanosponge from *A. aerophoba* were assessed *in vitro* using the standard disk diffusion method. Disk diffusion testing was performed in triplicate and according to the method described by Bauer et al. [33]. For the diffusion zone assay, pathogenic bacteria diluted to 0.5 McFarland turbidity were evenly inoculated onto Muller-Hinton Agar (MHA) using a sterile swab. Sterile discs (6 mm) loaded with 20 µL of the extract were then placed on the inoculated MHA, and the plates were incubated at 37 °C for 24 hours. Antimicrobial activity was evaluated by measuring the diameter of the inhibition zones formed around the discs.

The MIC was determined by using a microbroth dilution assay as previously described [34]. Briefly, the MIC was defined as the absence of visible colonies after incubating 10 µL of bacterial culture with a hybrid nanosponge containing *A. aerophoba* extract and Cu (II) ion (at concentrations of 0.25 to 1024 µg/mL) at 37 °C for 24 h. Wells containing only bacterial growth served as positive controls, and wells with MHB alone were used as negative controls. All

ARTICLE IN PRESS

antimicrobial experiments were performed in triplicate to ensure reproducibility.

2.5. Antioxidant Activity via DPPH Radical Scavenging Assay

The antioxidant potential of the Cu^{2+} hNSs synthesized using *A. aerophoba* extract was assessed through the 2,2-diphenyl-1-picrylhydrazyl (DPPH) free radical scavenging assay, following a well-established protocol [35]. Varying concentrations of hNFs, ranging from 0.165 mg/mL to 10 mg/mL, were prepared and added to a methanolic DPPH solution (0.1 mM). The reaction mixtures were incubated at room temperature in the dark for 30 minutes to prevent light-induced degradation of DPPH. The antioxidant activity was determined by measuring the decrease in absorbance at 517 nm, which corresponds to the reduction of the purple-colored DPPH radical to a yellow-colored non-radical form, indicative of radical scavenging. All assays were performed in triplicate to ensure reproducibility.

The results provided quantitative insight into the free radical scavenging capacity of the nanostructures, which is attributed to the bioactive constituents of the *A. aerophoba* extract and the synergistic effect of Cu(II) ions incorporated within the hybrid matrix.

The aforementioned calculation was performed as follows:

(1) Inhibition rate (%) = $(A_1 - A_2) \times 100/A_1$,

Where A_1 is the absorbance of the addition of ethanol to the test site and A_2 is the absorbance of the test sample solution [36,37].

3. Results and discussion

3.1. Synthesis and characterization of organic-inorganic hybrid nanosponge

Figure 1 depicts images obtained via scanning electron microscopy (SEM) of hNFs generated using *A. aerophoba* (1.65 mL) as the organic component when the phosphate-buffered saline (PBS) pH was 7.4. The diameter of the hNFs produced by utilizing 1.65 mL of *A. aerophoba* extract was found to be distributed between 12 and 14 µm (Fig. 1). The reported size range of 12–14 µm indeed refers to the aggregated structures observed in the SEM images,

ARTICLE IN PRESS

rather than the dimensions of the individual nanosponges. Due to their high surface energy and porous framework, nanosponges often undergo secondary agglomeration during sample preparation and drying, leading to microscale clusters.

Closer inspection of the morphology indicates that the individual nanosponge “petal-like” structures exhibit an average diameter of approximately 120–180 nm, which is consistent with the nanoscale dimensions typically reported for nanosponges. The synthesis of hNFs was divided into four phases by Li et al. [38]. The nucleation phase (step 1) is responsible for the formation of primary phosphate crystals, which occur as a result of the interaction between phosphate (PO_4^{3-}) and bivalent metals (Cu^{2+}, Ca^{2+}, Fe^{2+}, Mn^{2+}, etc.). The process of electrostatic binding is the interaction between negatively charged phosphate and positively charged bivalent metals. The interaction of primary phosphate crystals and amide/N groups of organic molecules results in the formation of nanopetals during the coordination and precipitation phase (steps 2 and 3). Anisotropic growth causes nanopetals to coalesce during the self-assembly stage (Step 4), which results in the formation of multi-layer hNFs. Until the nanocrystals have reached saturation, the kinetic and hierarchical synthesis of hNFs is carried out [38, 39]. The shape and dimensions of hybrid nanofibers (hNFs) are influenced by a multitude of parameters, including the organic and inorganic components, reaction duration, sonication, reaction temperature, and medium pH.

In previous investigations, the optimal synthesis medium pH values were identified for the synthesis of perfect hNFs [40, 41]. The results demonstrated that uniform hNFs with optimal floral shape could be generated when 1.65 mL of extract was added and the pH of the PBS buffer was 7.4. To provide concrete evidence, we refer to studies that have demonstrated similar dispersion characteristics in metal-doped nanosponges. For instance, Qiao et al. [42] reported that Cu-TCPP MOF sheets exhibit a smooth, uniform surface morphology, as observed in their SEM and TEM images, with EDX mapping confirming the homogeneous distribution of copper, nitrogen, and oxygen

ARTICLE IN PRESS

elements. Similarly, Xu et al. [43] demonstrated in $CuO@SiO_2$ nanocomposites nanocomposites that the organic copper precursor was uniformly dispersed throughout the silica matrix, as evidenced by SEM, TEM imaging, and EDX elemental maps showing even spatial distribution of Cu^{2+} ions. Our findings are consistent with those of previous research, which has employed hNFs produced under ideal circumstances for investigations into catalysis and antioxidants. Similar marine-derived biomaterials, such as alginates and sponge/fungal metabolites, have also been employed in nanostructure synthesis, further supporting the potential of sponge extracts as organic templates [13-15].

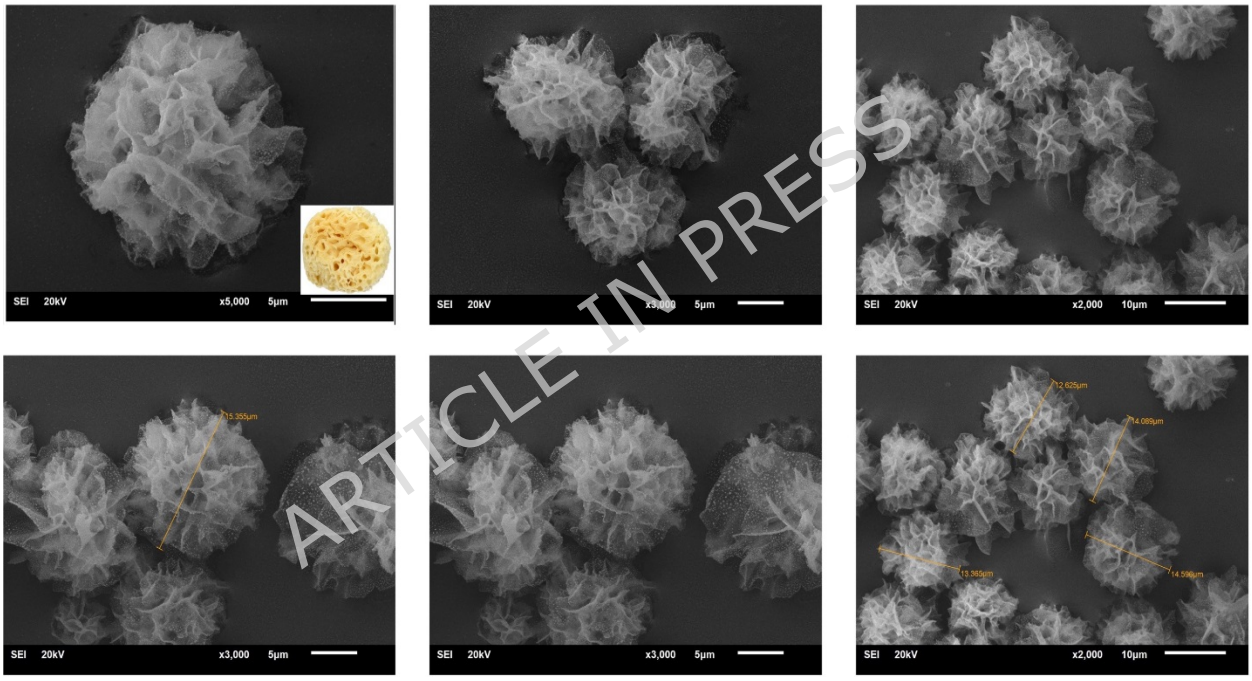


Figure 1. SEM image of Cu(II) ion-incorporated *Aplysina aerophoba* hybrid nanosponge (~12–14 µm) showing porous morphology.

The results of the EDX analysis and EDX mapping indicate that the Cu and other elemental components (C, O, Na, N, and P) present in the structure of the hNFs synthesized using *A. aerophoba* as an organic component are displayed, respectively (Fig. 2). The percentage weights of the elements C, O, Na, Cu, N, and P found in hNFs were found to be 37.4, 32.0, 11.4, 9.7, 5.6, and

ARTICLE IN PRESS

3.9%, respectively. Moreover, the atomic percentage values of hNFs are presented in Fig. 7 and are given as 69.72, 25.78, 2.01, and 2.50, respectively.

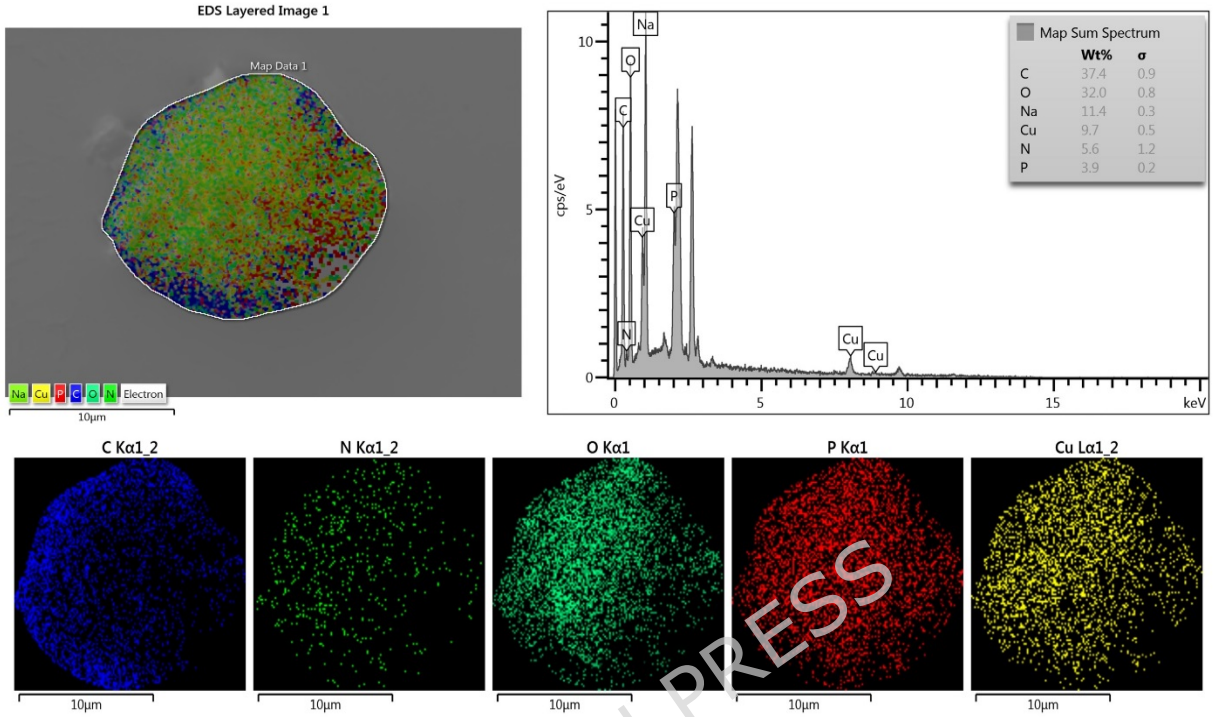


Figure 2. EDX spectra and elemental mapping of Cu(II) ion-incorporated *Aplysina aerophoba* hybrid nanosponge showing copper and other key elements.

ARTICLE IN PRESS

The functional groups present in the structure of Cu^{2+} hNSs were identified through the observation of vibrations in the FT-IR diagram (Fig. 3). The completion of the Cu(II) ion-incorporated *A. aerophoba* hybrid nanosponge synthesis was confirmed by FTIR analysis, where the disappearance of free –OH stretching vibrations of cyclodextrin and the appearance of new absorption bands associated with ester/carbonate linkages indicated successful crosslinking. These findings are consistent with previous reports confirming reaction completion in nanosponge synthesis through FTIR and complementary techniques such as XRD and TGA [44-48]. The presence of aromatic rings (C = C) and aliphatic ether (C–O) in the structure of hNFs was determined by the observation of peaks at 1615 cm^{-1} and 1176 cm^{-1},

ARTICLE IN PRESS

respectively. The presence of primary phosphate was revealed by the observation of vibrations at 1110 cm^{-1}, 1037 cm^{-1}, 892 cm^{-1}, 846 cm^{-1}, and 735 cm^{-1} [35, 40]. The X-ray diffraction (XRD) peaks, as illustrated in Figure 4, were identified at 2θ = 9.21°, 13.16°, 18.7°, 20.42°, 24.15°, 30.76°, 34.11°, 37.28°, 41.52°, 45.96°, 54.08°, and 56.21°, corresponding to $Cu_3(PO_4)_2$ crystals. XRD peaks were indexed using the appropriate JCPDS cards (Cu_2O: 05-0667), and the (hkl) plane labels were added to the diffractograms. The average crystallite size (D) was estimated from representative reflections using the Debye–Scherrer equation $D=K\lambda/(\beta\cos\theta)$, with K=0.9 and λ=0.15406 nm (Cu Kα). After correcting the measured FWHM for instrumental broadening, the calculated D values from multiple peaks yielded an average crystallite size of ~30 nm, consistent with the nanoscale domains inferred from microscopy.

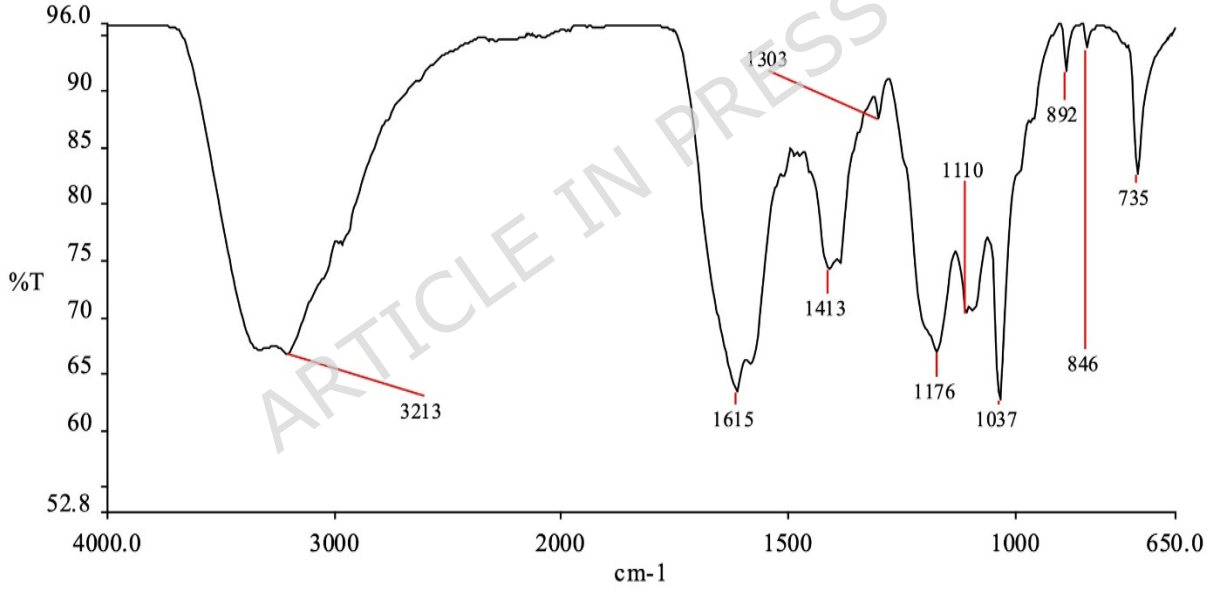


Figure 3. FT-IR spectra of Cu(II) ion-incorporated *Aplysina aerophoba* hybrid nanosponge, showing characteristic functional groups.

ARTICLE IN PRESS

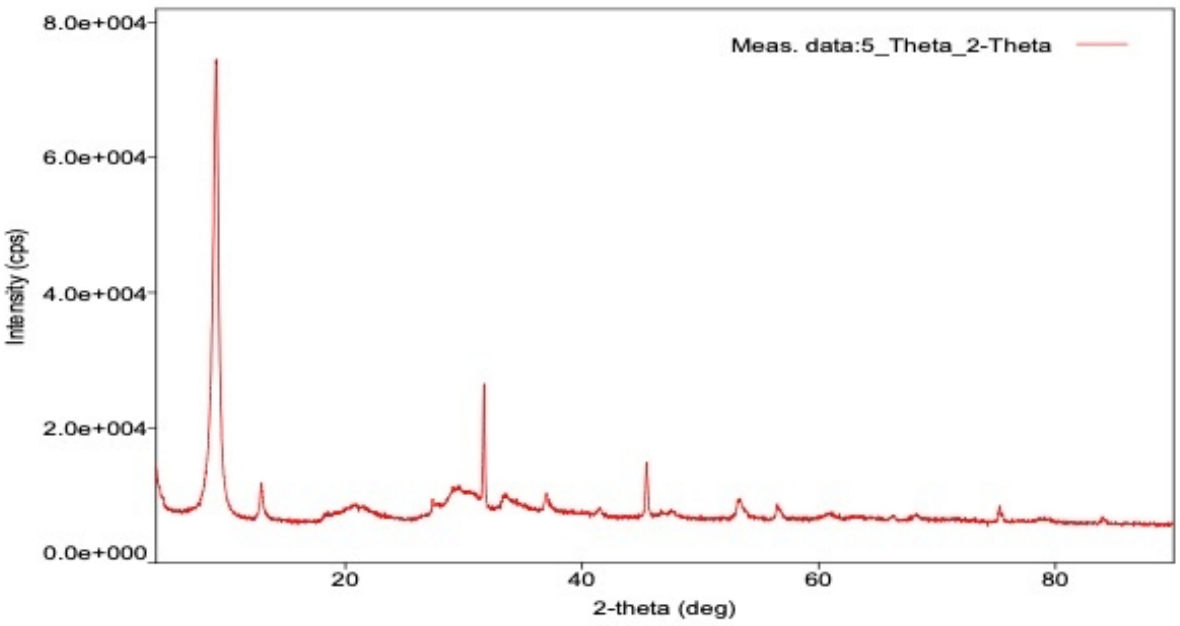


Figure 4. XRD patterns of Cu(II) ion-incorporated *Aplysina aerophoba* hybrid nanosponge, showing crystalline structure and copper incorporation.

3.2. Analysis of antioxidant activity

Antioxidants represent a vital resource for the prevention of oxidative stress-related damage. In the DPPH structure, unpaired electrons accept electrons from the oxidants, thereby stabilizing the system. A spectrophotometer reading at 517 nm is employed to quantify the colorimetric changes that oxidants induce in DPPH by transferring electrons to the compound [49]. Figure 5 illustrates the antioxidant activity of hNSs in the presence of *A. aerophoba* extract against DPPH. *A. aerophoba* extracts were prepared using ethanol and water, and the DPPH assay was employed to assess their antioxidant capacity. The results indicated that the Cu^{2+} hNSs themselves exhibited no measurable antioxidant activity, whereas the ethanol and aqueous extracts of *A. aerophoba* achieved approximately 13% DPPH radical reduction. In comparison, ascorbic acid demonstrated markedly higher activity, with 84.1% scavenging in water and 80% in ethanol.

By the findings above, a previous study has demonstrated that, contingent on concentration, iron NFs and nanocubes exhibit DPPH scavenging activity [50].

ARTICLE IN PRESS

A study by Altinkaynak et al. [51] found that Cu^{2+} hNSs based on *Aloe vera* extract and *A. vera* extract exhibited similar antioxidant properties. Bivalent metal-based nanocrystals (Co, Zn, and Cu) coordinated with amino acids were also reported to display stronger DPPH scavenging capacity compared to amino acid@bivalent metal hNFs [52]. Furthermore, the authors posit that among the various hNFs that coordinate the coordination of amino acids (histidine, cysteine, asparagine, and aspartic acid) and bivalent metals (Co, Zn, and Cu), cysteine@Zn hNFs exhibit the most pronounced antioxidant activity against DPPH. It was observed in the study that the hNFs produced exhibited antioxidant properties, preventing oxidative damage and free radical formation. Prior research has demonstrated that the organic and inorganic component varieties and concentrations of hNFs have a significant impact on their DPPH scavenging activities.

The absence of antioxidant activity in Cu(II)-incorporated hybrid nanosponges synthesized by green methods may be attributed to several factors. Copper ions (particularly in the Cu^{2+} state) can participate in Fenton-like reactions, generating reactive oxygen species (ROS) and exerting a pro-oxidant effect. In addition, the bioactive compounds present in plant extracts may degrade or become encapsulated during synthesis, thereby reducing their accessibility and contribution to antioxidant function [53]. Furthermore, the morphology and limited surface area of the nanostructure may hinder effective radical scavenging interactions. Together, these factors, along with possible incompatibility between the DPPH assay and the physicochemical properties of the nanomaterials, may explain the lack of observable antioxidant activity in Cu^{2+} hNSs. By contrast, several marine-derived biopolymers have been reported to retain strong antioxidant activity in nanostructures, suggesting that the incorporation of Cu^{2+} may suppress these beneficial effects [13, 14]. This interpretation is consistent with recent reviews highlighting the pro-oxidant behaviour of CuO nanoparticles [29].

ARTICLE IN PRESS

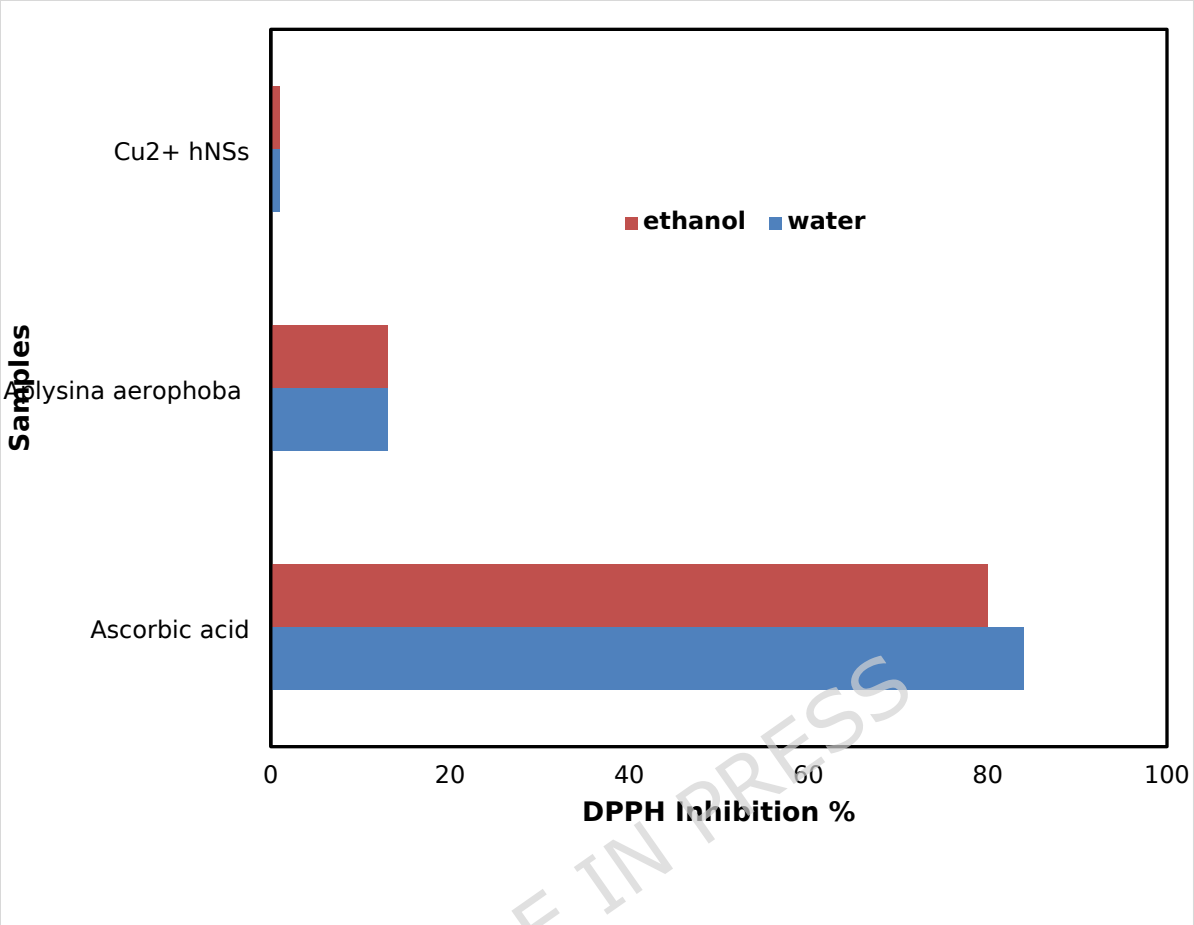


Figure 5. DPPH radical scavenging activity of *Aplysina aerophoba* extract and Cu(II) ion-incorporated hybrid nanosponge.

ARTICLE IN PRESS

3.3. Analysis of antimicrobial activity

The inhibition zone and minimum inhibition concentration of *A. aerophoba* extract and Cu(II) ion hybrid nanosponges (Cu^{2+} hNSs) against pathogen bacteria are presented in Figure 6 and Table 1, respectively. According to the results of antibacterial susceptibility tests, no effect of the *A. aerophoba* extract was observed against *A. sobria, S. aureus*, *E. coli*, *S. enterica*, and *A. hydrophila*. *A. aerophoba* extract had antibacterial activity only on *A. hydrophila* with a MIC of 1024 µg/mL (Table 1). In contrast, incorporation of Cu^{2+} ions markedly enhanced antibacterial efficacy across all strains tested. Cu^{2+} hNSs produced inhibition zones of 15.17 mm (*A. sobria*), 18.67 mm (*S. enterica*), 22.03 mm (*E. coli*), 31.43 mm (*A. hydrophila*) and 31.46 mm (*S.*

ARTICLE IN PRESS

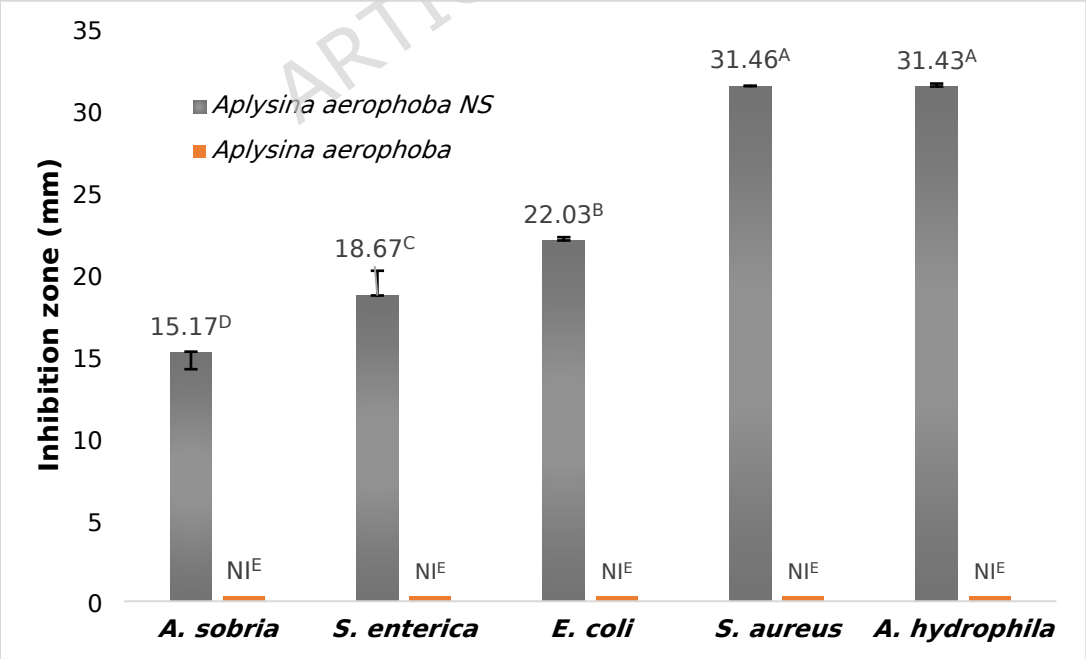
aureus), with corresponding MIC values ranging from 16–128 µg/mL (Figure 6). Statistical analysis demonstrated that the inhibition zones of *S. aureus* and *A. hydrophila* were not significantly different from each other ($p > 0.05$). In contrast, those of *A. sobria*, *S. enterica,* and *E. coli* each differed significantly from one another and the former pair ($p < 0.05$). Similarly, the MIC values obtained for Cu^{2+} hNSs (16–128 µg/mL) were significantly lower than that of the crude extract, which exhibited activity only against *A. hydrophila* with a MIC of 1024 µg/Ml (Table 1). These findings confirm that Cu^{2+} hNSs exhibit significantly higher antimicrobial activity than the extract alone. This pattern is consistent with recent reports on Cu-based nanomaterials (CuO/Cu_2O NPs and copper composites), which highlight broad-spectrum antibacterial and antibiofilm effects and improved efficacy versus crude extracts or matrices [29-31]. Taken together, our data suggest that the marine-derived organic framework of the sponge extract synergizes with copper to enhance activity at lower MIC ranges, which is comparable to the ranges summarized in recent reviews.

The interaction mechanism of Cu^{2+} hNSs with bacteria is not yet well known. However, incorporation of Cu^{2+} ions is likely responsible for the enhanced antimicrobial activity compared to the crude extract. Cu^{2+} ions may interact electrostatically with negatively charged bacterial cell membranes, leading to membrane disruption and leakage of intracellular contents. Furthermore, Cu^{2+} can undergo redox cycling (Cu^{2+}/Cu^{+}) in the presence of H_2O_2, generating hydroxyl radicals (•OH) that damage proteins, lipids, and DNA, thereby amplifying bactericidal effects [20,54]. These mechanisms together may explain why Cu^{2+} hNSs exhibit significantly stronger antibacterial activity than the extract alone. Similarly, Altinkaynak et al. [55] reported that Cu^{2+} hNFs exhibited higher antimicrobial activity than normal extract against some Gram-positive and Gram-negative bacteria. Another study reported that NF synthesis from plant extracts improved antimicrobial activity against *E. coli*, *S. typhi*, *P. aeruginosa*, *S. aureus* and *C. albicans* compared to extracts [56].

ARTICLE IN PRESS

However, some potential disadvantages of the Cu^{2+} hNSs should be noted. These nanoparticles may exhibit cytotoxicity at higher concentrations toward mammalian cells [57], face stability issues such as aggregation or oxidation over time [58] and show a limited spectrum of activity against untested bacterial strains [29]. Additionally, the release kinetics of copper ions or bioactive compounds may not be fully controllable, potentially affecting antimicrobial efficiency [59]. Finally, the use of copper-containing nanoparticles raises possible environmental concerns if not properly managed [60]. Similar concerns about toxicity, stability, and environmental impact have also been emphasized in recent comprehensive reviews of Cu-based nanomaterials [30,31]. This study demonstrates that Cu(II)-doped hybrid nanosponges functionalized with *A. aerophoba* extract exhibit enhanced stability and bioactive performance. These findings provide a cost-effective and versatile nanosponge platform with potential applications in nanomedicine, pharmaceuticals, and nutraceuticals. Researchers, healthcare sectors, and industry can benefit from this approach as a strategy for developing multifunctional carriers for antimicrobials, and other bioactives.

ARTICLE IN PRESS



ARTICLE IN PRESS

Figure 6. Antibacterial activity of *Aplysina aerophoba* extract and Cu(II) ion-incorporated hybrid nanosponge (NS) against pathogenic bacteria. Different superscript letters above the bars indicate statistically significant differences ($p < 0.05$). NI: No inhibition zone.

ARTICLE IN PRESS

ARTICLE IN PRESS

Table 1. Minimum inhibitory concentration (MIC, μg/mL) of *Aplysina aerophoba* extract and Cu(II) ion-incorporated hybrid nanosponge (NS) against pathogenic bacteria.

Extracts	*A. sobria*	*S. enterica*	*E. coli*	*S. aureus*	*A. hydrophila*
A. aerophoba	**+**	**+**	**+**	**+**	**1024**
***A. aerophoba* NS**	**128**	**128**	**128**	**64**	**16**

4. Conclusion

In this study, Cu^{2+} ions were coordinated with *A. aerophoba* extract under mild conditions (room temperature, pH 7.4) to fabricate hNSs via a self-assembly process. Overall, this work establishes a reliable strategy for designing metal-doped, biofunctionalized nanosponges with controlled morphology and enhanced bioactive performance. The hybrid nanostructures (hNSs) synthesized in this study displayed natural antibacterial effects. The green synthesis method used—a simple, low-cost, and environmentally friendly process—provides a sustainable alternative to traditional techniques for producing nanomaterials. Due to their biocompatibility and multifunctional nature, these hNSs are well-suited for various biomedical uses, such as drug delivery, wound healing, antimicrobial surface treatments, and antioxidant therapies. In addition, this synthesis approach can be adapted to other natural sources like algae, fungi, or plants, allowing the design of nanostructures for targeted clinical applications. In addition to demonstrating enhanced structural stability and bioactivity, the green self-assembled synthesis of Cu(II)-doped hybrid nanosponges offers a cost-effective and environmentally friendly alternative to conventional chemical and physical methods.

By utilizing *A. aerophoba* extract as a natural reducing and stabilizing agent under mild reaction conditions, this approach minimizes reagent costs, energy consumption, and post-synthetic processing, while simultaneously achieving biofunctionalization. These features make the method attractive for

ARTICLE IN PRESS

laboratory-scale applications and provide a foundation for potential scale-up in pharmaceutical, nutraceutical, and biomedical fields.

Acknowledgements

The authors are thankful for the services and facilities of The Technology Research and Implementation Centre of Recep Tayyip Erdogan University.

Author Contributions

Ayse DEMİRBAS: Planning of the study, synthesis, characterization of nanosponges, antioxidant activity of nanosponges and *A. aerophoba* extract, writing and editing. Baris KARSLI: Antimicrobial activity of nanosponges, methodology, writing. İbrahim Seyda URAS and Belma KONUKLUGİL: Collecting and extracting of *A. aerophoba*.

Funding

Not applicable

Data Availability Statement

All data supporting the findings of this study are included within the article.

Conflict of Interest

The authors have declared that no competing interests exist.

Ethics declaration: not applicable

References

[1] Van Soest, R. *Aplysina aerophoba*. Sponges of the NE Atlantic. Marine Species Identification Portal. https://species-identification.org (accessed 22 September 2020).

[2] Kreuzberg, R. Yellow tube sponge: *Aplysina aerophoba*. Tauchen auf den Kanaren. https://www.tauchen-kanaren.de (accessed 22 September 2020).

[3] Ehrlich, H. et al. Three dimensional chitin–based scaffolds from Verongida sponges (Demospongiae: Porifera). Part I. Isolation and identification of chitin. *Int. J. Biol. Macromol*. **47**, 132–140 (2010).

[4] Ehrlich, H., Bazhenov, V. V., Meschke, S., Bürger, M., Ehrlich, A., Petovic, S. et al. Marine invertebrates of Boka Kotorska Bay unique sources for bioinspired materials science. In: Djurović, M., Semenov, A. V., Zonn, I. S. & Kostianoy, A. G. (eds) *The Boka Kotorska Bay Environment*. *The Handbook of Environmental Chemistry*. 313–334 (Springer, 2016).

[5] Bechmann, N. et al. Anti–tumorigenic and anti–metastatic activity of the sponge–derived marine drugs Aeroplysinin–1 and Isofistularin–3 against pheochromocytoma *in vitro*. *Mar. Drugs* **16**, 172 (2018).

ARTICLE IN PRESS

[6] Ebel, R., Brenzinger, M., Kunze, A., Gross, H. J. & Proksch, P. Wound activation of protoxins in marine sponge *Aplysina aerophoba*. *J. Chem. Ecol.* **23**, 1451–1462 (1997).
[7] Thoms, C., Wolff, M., Padmakumar, K., Ebel, R. & Proksch, P. Chemical defense of Mediterranean sponges *Aplysina cavernicola* and *Aplysina aerophoba*. *Z. Naturforsch. C* **59**, 113–122 (2004).
[8] Orfanoudaki, M. *et al.* Cytotoxic compounds of two demosponges (*Aplysina aerophoba* and *Spongia* sp.) from the Aegean Sea. *Biomolecules* **11**, 723 (2021).
[9] Koulman, A. *et al.* Cytotoxicity and mode of action of aeroplysinin-1 and a related dienone from the sponge *Aplysina aerophoba*. *J. Nat. Prod.* **59**, 591–594 (1996).
[10] Binnewerg, B. et al. Marine biomaterials: Biomimetic and pharmacological potential of cultivated *Aplysina aerophoba* marine demosponge. *Mater. Sci. Eng. C* **109**, 110566 (2020).
[11] Çankırılıgil, E. & Berik, N. A preliminary study on the antioxidant activity and amino acid composition of marine sponge *Aplysina aerophoba* collected from Northeastern Aegean Sea. In *5th National Marine Sciences Conference*; Turkey, 2022.
[12] Carnovali, M. *et al.* Aerophobin-1 from the marine sponge *Aplysina aerophoba* modulates osteogenesis in zebrafish larvae. *Mar. Drugs* **20**, 135 (2022).
[13] Kokova, V., Lukova, P., Baldzhieva, A., Katsarov, P., Delattre, C., Molinié, R., Petit, E., Elboutachfaiti, R., Murdjeva, M. & Apostolova, E. Extraction, structural characterization, and *in vivo* anti-inflammatory effect of alginate from *Cystoseira crinita* (Desf.) Borry harvested in the Bulgarian Black Sea. *Mar. Drugs* **21**, 245 (2023).
[14] Shin, H. J., Lee, M. A., Lee, H.-S. & Heo, C.-S. Thiolactones and Δ8,9-pregnene steroids from the marine-derived fungus *Meira* sp. 1210CH-42 and their α-glucosidase inhibitory activity. *Mar. Drugs* **21**, 246 (2023).
[15] Khiari, Z. Recent developments in bio-ink formulations using marine-derived biomaterials for three-dimensional (3D) bioprinting. *Mar. Drugs* **22**, 134 (2024).
[16] Cui, J., Zhao, Y., Liu, R. et al. Surfactant-activated lipase hybrid nanoflowers with enhanced enzymatic performance. *Sci. Rep.* **6**, 27928 (2016).
[17] Cui, J. & Jia, S. Organic–inorganic hybrid nanoflowers: A novel host platform for immobilizing biomolecules. *Coord. Chem. Rev.* **352**, 249–263 (2017).
[18] Wen, H. et al. Bimetal based inorganic–carbonic anhydrase hybrid hydrogel membrane for CO_2 capture. J*. CO_2 Util.* **39**, 101171 (2020).
[19] Hussain, I., Singh, N. B., Singh, A., Singh, H. & Singh, S. C. Green synthesis of nanoparticles and its potential application. *Biotechnol. Lett.* **38**, 545–560 (2016).

ARTICLE IN PRESS

ARTICLE IN PRESS

[20] Demirbas, A. Comparison study of synthesized red (or blood) orange peels and juice extract-nanoflowers and their antimicrobial properties on fish pathogen (*Yersinia ruckeri*). *Indian J. Microbiol.* **61**, 324–330 (2021).
[21] Ekennia, A. C. et al. Green synthesis of biogenic zinc oxide nanoflower as dual agent for photodegradation of an organic dye and tyrosinase inhibitor. *J. Inorg. Organomet. Polym. Mater.* **31**, 886–897 (2020).
[22] Al Sharie, A. H. et al. Green synthesis of zinc oxide nanoflowers using *Hypericum triquetrifolium* extract: characterization, antibacterial activity and cytotoxicity against lung cancer A549 cells. *Appl. Organomet. Chem.* **34**, e5667 (2020).
[23] Karsli, B., Uras, I. S., Konuklugil, B. & Demirbas, A. Synthesis of *Axinyssa digitata* extract directed hybrid nanoflower and investigation of its antimicrobial activity. *IEEE Trans. Nanobiosci.* **22**, 523–528 (2023).
[24] Shahabadi, N. et al. Green synthesis of chloroxine-conjugated silver nanoflowers: Promising antimicrobial activity and *in vivo* cutaneous wound healing effects. *J. Environ. Chem. Eng.* **9**, 105215 (2021).
[25] Uras, I. S., Karsli, B., Konuklugil, B., Ocsoy, I. & Demirbas, A. Organic–inorganic nanocomposites of *Aspergillus terreus* extract and its compounds with antimicrobial properties. *Sustainability* **15**, 4638 (2023).
[26] Demirbas, A. et al. *Usnea antarctica* and *Usnea subfloridana* incorporated hybrid nanoflowers with their intrinsic catalytic and antimicrobial activities. *ChemistrySelect* **7**, e202202715 (2022).
[27] Koca, F. D., Muhy, H. M. & Halici, M. G. Catalytic and antioxidant activity of *Desmarestia menziesii* algae extract based organic@inorganic hybrid nanoflowers. *J. Inorg. Organomet. Polym. Mater.* **34**, 1282-1292 (2024).
[28] González-Ballesteros, N., González-Rodríguez, J. B., Rodríguez-Argüelles, M. C. & Lastra, M. J. P. S. New application of two Antarctic macroalgae *Palmaria decipiens* and *Desmarestia menziesii* in the synthesis of gold and silver nanoparticles. *Polar Sci.* **15**, 49–54 (2018).
[29] Gudkov SV, Burmistrov DE, Fomina PA, Validov SZ, Kozlov VA. Antibacterial properties of copper oxide nanoparticles (Review). *Int J Mol Sci*. **25**, 11563 (2024).
[30] Wei Q, Pan Y, Zhang Z, Yan S, Li Z. Copper-based nanomaterials for biomedical applications. *Chem Eng J.* **483**, 149040 (2024).
[31] Wang Y, Wen T, Mao F, Yang S, Zhang Q, Fu X, Zhang H. Engineering copper and copper-based materials for a post-antibiotic era. *Front Bioeng Biotechnol.* **13**, 1644362 (2025).
[32] Karslı, B. Antibacterial and antioxidant activity of pulp, peel and leaves of *Feijoa sellowiana*: Effect of extraction techniques, solvents and concentration. *Food Health* **7**, 21–30 (2021).
[33] Bauer, A. W., Kirby, W. M., Sherris, J. C. & Turck, M. Antibiotic susceptibility testing by a standardized single disk method. *Am. J. Clin. Pathol.* **45**, 493–496 (1966).
[34] Ildiz, N., Baldemir, A., Altinkaynak, C., Ozdemir, N., Yilmaz, V. & Ocsoy, I. Self assembled snowball-like hybrid nanostructures comprising *Viburnum*

ARTICLE IN PRESS

opulus L. extract and metal ions for antimicrobial and catalytic applications. *Enzyme Microb. Technol.* **102**, 60–66 (2017).
[35] Güven, O. C., Kar, M. & Koca, F. D. Synthesis of cherry stalk extract based organic@inorganic hybrid nanoflowers as a novel fenton reagent: evaluation of their antioxidant, catalytic, and antimicrobial activities. *J. Inorg. Organomet. Polym. Mater.* **32**, 1026–1032 (2022).
[36] Demirbas, A. et al. Preparation of biocompatible and stable iron oxide nanoparticles using anthocyanin integrated hydrothermal method and their antimicrobial and antioxidant properties. *Mater. Res. Express* **6,** 125011 (2019).
[37] Xiao, F., Xu, T., Lu, B. & Liu, R. Guidelines for antioxidant assays for food components. *Food Front.* **1**, 60–69 (2020).
[38] Li, Y., Wu, H. & Su, Z. Enzyme-based hybrid nanoflowers with high performances for biocatalytic, biomedical, and environmental applications. *Coord. Chem. Rev.* **416**, 213342 (2020).
[39] Chen, J. et al. Organic–inorganic hybrid nanoflowers: A comprehensive review of current trends, advances, and future perspectives. *Coord. Chem. Rev.* **489**, 215191 (2023).
[40] Alhayali, N. I., Özpozan, N. K., Dayan, S., Özdemir, N. & Somtürk Yılmaz, B. Catalase/Fe_3O_4@Cu^{2+} hybrid biocatalytic nanoflowers fabrication and efficiency in the reduction of organic pollutants. *Polyhedron* **194**, 114888 (2021).
[41] Celik, C., Ildiz, N. & Ocsoy, I. Building block and rapid synthesis of catecholamines-inorganic nanoflowers with their peroxidase-mimicking and antimicrobial activities. *Sci. Rep*. **10**, 2903 (2020).
[42] Qiao X, Arsalan M, Ma X, et al. A hybrid of ultrathin metal–organic framework sheet and ultrasmall copper nanoparticles for detection of hydrogen peroxide with enhanced activity. *Anal Bioanal Chem*. **413**, 839–851 (2021).
[43] Xu L, Zhang J, Li Z, Ma Q, Wang Y, Cui F, Cui T. In situ generation of ultrasmall sized and highly dispersed CuO nanoparticles embedded in silica matrix and their catalytic application. *New J Chem*. **43**, 520-526 (2019).
[44] Swaminathan S, Cavalli R, Trotta F. Cyclodextrin-based nanosponges: A versatile platform for cancer nanotherapeutics development. *Wiley Interdiscip Rev Nanomed Nanobiotechnol*. **8**, 579-601 (2016).
[45] Vinay SP, Udayabhanu, Nagaraju G, Chandrappa CP, Chandrasekhar N. A novel, green, rapid, nonchemical route hydrothermal assisted biosynthesis of Ag nanomaterial by blushwood berry extract and evaluation of its diverse applications. *Appl Nanosci*. **10**, 3341-3351 (2020).
[46] Vinay SP, Sumedha HN, Shashank M, Nagaraju G, Chandrasekhar N. In-vitro antibacterial, antioxidant and cytotoxic potential of gold nanoparticles synthesized using novel *Elaeocarpus ganitrus* seeds extract. *J Sci Adv Mater Devices*. **6**, 127-133 (2021).
[47] Deze EG, Bareka MD, Karousos DS, Sapalidis AA, Favvas EP. Mesoporous silica based copper catalytic materials for potential deNOx application: Synthesis and characterization. *Mater Today Proc*. **54**, 1–6 (2022).

ARTICLE IN PRESS

[48] Utzeri G, Matias PMC, Murtinho D, Valente AJM. Cyclodextrin-based nanosponges: Overview and opportunities. *Front Chem*. **10**, 859406 (2022).
[49] Sumra, A. A. et al. Biogenic synthesis, characterization, and *in vitro* biological evaluation of silver nanoparticles using *Cleome brachycarpa*. *Plants* **12**, 1578 (2023).
[50] Eskikaya, O. et al. A comparative study of iron nanoflower and nanocube in terms of antibacterial properties. *Appl. Nanosci*. **13**, 5421–5433 (2023).
[51] Altinkaynak, C. et al. Anti-microbial, anti-oxidant and wound healing capabilities of *Aloe vera*-incorporated hybrid nanoflowers*. J. Biosci. Bioeng*. **135**, 321–330 (2023).
[52] Özdemir, N., Altinkaynak, C., Türk, M., Geçili, F. & Tavlaşoğlu, S. Amino acid-metal phosphate hybrid nanoflowers (AaHNFs): their preparation, characterization and anti-oxidant capacities. *Polym. Bull.* **79**, 9697-9716 (2022).
[53] Andrés, C. M. C., Pérez de la Lastra, J. M., Juan, C. A., Plou, F. J. & Pérez-Lebeña, E. Polyphenols as antioxidant/pro-oxidant compounds and donors of reducing species: Relationship with human antioxidant metabolism. *Processes* **11**, 2771 (2023).
[54] Ahmed, S., Ahmad, M., Swami, B. L. & Ikram, S. A review on plants extract mediated synthesis of silver nanoparticles for antimicrobial applications: A green expertise. *J. Adv. Res.* **7**, 17–28 (2016).
[55] Altinkaynak, C. et al. Synthesis of organic-inorganic hybrid nanoflowers using *Trigonella foenum-graecum* seed extract and investigation of their antimicrobial activity. *Derim* **36**, 159–167 (2019).
[56] Kilic, A. B. et al. A new approach for green synthesis and characterization of *Artemisia* L. genotype extracts–Cu^{2+} nanocomplexes (nanoflower) and their effective antimicrobial activity. *Medicine* **9**, 191–196 (2020).
[57] Alarifi, S., Ali, D., Verma, A., Alakhtani, S. & Ali, B. A. Cytotoxicity and genotoxicity of copper oxide nanoparticles in human skin keratinocytes cells. *International Journal of Toxicology* **32**, 296–307 (2013).
[58] Tegenaw, A., Sorial, G. A., Sahle-Demessie, E. & Han, C. Role of water chemistry on stability, aggregation, and dissolution of uncoated and carbon-coated copper nanoparticles. *Environmental Research* **187**, 109700 (2020).
[59] Gunawan, C., Teoh, W. Y., Marquis, C. P. & Amal, R. Cytotoxic origin of copper(II) oxide nanoparticles: Comparative studies with micron-sized particles, leachate, and metal salts. *ACS Nano* **5**, 7214–7225 (2011).
[60] Tortella, G. et al. Copper nanoparticles as a potential emerging pollutant: Divergent effects in the agriculture, risk–benefit balance and integrated strategies for its use. *Emerging Contaminants* **10**, 100352 (2024).